Experimental study of deposit morphology and sediment transport in a flume

J. Dreano & A. Valance
Institut de Physique de Rennes, Rennes, FRANCE

C. Cassar & D. Lague
Géosciences Rennes, Rennes, FRANCE

ABSTRACT: We studied experimentally the development of bedform instabilities on a rough non-erodible bed as a function of the rate of sediment supplied, and the coupling between the morphodynamics of the bed deposits and the various modes of sediment transport. The experimental setup is a rectangular closed duct that combines an innovative system to control precisely the rate of sediment supply Q_{in}, a digitizing system to measure in real-time the 3D bed topography, and a 2D particle tracking system to compute concentration profiles. We show that for each rate of sediment supply, the bedform instabilities (barchans, transverse dunes) reach a steady-state geometry after a timescale decreasing with Q_{in}. Steady-state bedform elevation increases with Q_{in} while migration speed is surprisingly constant. To better understand these observations, we studied how the flux of sediment transport is partitioned between bedload, suspended-load and bedform advection flux. As Q_{in} increases, the bedload part increases significantly to become the dominant regime (~ 80 %). These results show that the sediment availability, in addition to flow conditions, plays a crucial role in the morphology dynamics of the bedforms and in the partition between the different modes of transport.

1 INTRODUCTION

Dynamics and laws which govern sediment transport and deposition in rivers are still misunderstood. The difficulty to progress on this topic arises from the complexity of the coupling between the development of bedform instabilities, the retroaction on fluid dynamics and sediment transport. For instance, it is difficult to predict precisely the proportion of sediment supplied to a non-erodible channel that will be transported as bedload, suspended-load or via the migration of bed deposits. Yet, this has a lot of implications from river management issues (Church et al. 1998) to fundamental research on the dynamics of river and landscape evolution at geological timescales (Turowski et al. 2007). Given the difficulty to get good in situ data combining both fluxes and bed morphology, experimental approaches in laboratory using flumes are therefore essential. It allows to control the parameters characterizing the natural complexity of rivers (temporal and geometrical aspects), and to investigate their respective influence on the transport and deposition processes. There are many experimental studies concerning the formation of bedforms on erodible soils submitted to water flow (Ouriemi 2007, Langlois 2005, Charru et al. 2004).
But there are few experiments investigating the deposition process on rigid (non erodible) soils (Endo et al. 2005). We thus developed an experimental flume in which sediment supply rate can be precisely set and bed topography digitized in almost real-time to study how bed deposits and sediment transport co-develop. We studied in particular the timescales of bedforms development and the relationships between rate of sediment supplied, bedforms geometry and the mode of sediment transport (bedload, suspended-load and bedform migration).

2 EXPERIMENTAL SETUP AND PROTOCOL

2.1 *Experimental setup*

Experiments were performed in a rectangular closed flume. The flume is 3 m long, 120 mm wide and 75 mm deep (Fig. 1). Thanks to a rectilinear substrate laid at the bottom of the flume, the cross section in the working area is reduced to 35 mm high and 120 mm wide. Water flow is generated by gravity and a valve controls the flow rate. The cover and the walls of the flume are transparent to ease the observation of flow and sediment. At the entrance of the channel, a system ensures a constant and controlled sediment discharge into the flume, which can be tuned independently of the water discharge. 20 cm further down stream, the surface of the substrate is made

rough by gluing spherical beads on it over a distance of 1m. At the end of the channel, water was filtered and returned to the tank by means of a pump. Sediments used were glass beads well sorted, 100 µm in diameter and 2.5 g/cm^3 in density.

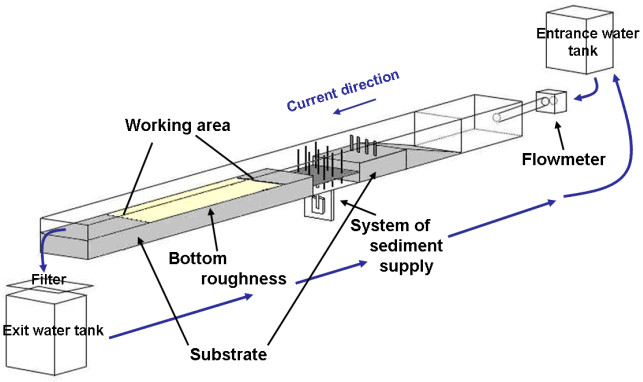

Figure 1. Experimental setup.

2.2 *Experimental protocol*

At the beginning of each experiment, the sediment supply system is filled up with glass beads. Then, sediment discharge was adjusted and kept constant for the whole duration of the experiment. We carried out a set of experiments at a given water flow rate varying the sediment flow rates. The water flow rate was fixed at 71 L/min for all experiments. The shear velocity measured above the rough bottom is 2.6 cm/s, the corresponding Shields number is 0.4 and the Reynolds number is 14000.

We performed two types of measurements. The first type of measurements concerned the morphology of the sediment deposit on the rough part of the channel. For these morphological measures, a system using Moiré principle was used (Breque and al. 2004). The 3D topography of the deposits was therefore obtained. The second type of measurements dealt with the estimation of the different modes of sediment transport (bedload, suspension, …). In particular, we measured, by means of a particle tracking system, the flux of suspended sediment particles.

These two types of measurements were repeated at regular time intervals (Δt = 30 s for the Moiré system, and Δt = 100 to 400 s for the particle tracking system) during the whole duration of the experiment. We therefore had access to the temporal evolution of the sediment deposit pattern and of the suspended sediment flux.

2.3 *System of sediment supply*

The system of sediment supply consists in a metal rod coming through the bottom of the channel. At the lower end, the rod is linked to a step-by-step motor, whom we control the velocity. This motor allows a vertical displacement of the metal rod. A horizontal plate, 5 mm thick, 120 mm wide and long, is fixed at the upper end of the metal rod. Several holes were bored in the plate to allow Teflon bars going through. These bars, whose role is explained later on, are quenched between the bottom and the cover of the channel, so that the plate can move upwards or downwards while the bars are kept fixed (Fig. 2).

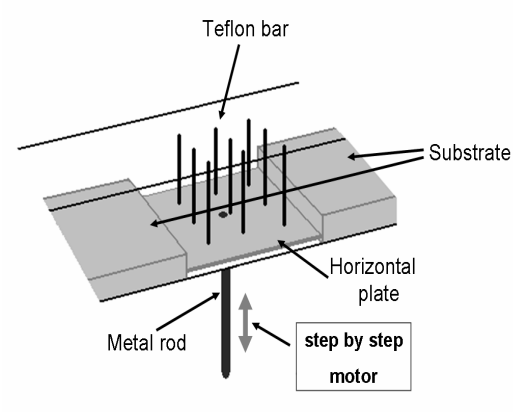

Figure 2. System of sediment supply.

At the beginning of an experiment, the plate lies at the bottom of the flume, and is therefore below the level of the substrate. The cavity is filled up with glass beads up to the level of the substrate. The rising velocity of the horizontal plate, V_{up}, is controlled via the frequency of the step-by-step motor. As the plate rises, sediment is eroded by the water flow and transported into the flume. In the erosion process, the presence of the Teflon bars is crucial: they ensure a homogeneous erosion of sediment on the supply area. In particular, they prevent the formation of a dune which would give an inhomogeneous erosion. The bed surface of the supply system remains flat. The injected vertical sediment rate Q_{in} can be estimated as follows:

$$Q_{in} = V_{up} \times \rho_{beads} \times \Phi \times l \quad (1)$$

where ρ_{beads} is the glass beads density, Φ the solid volume fraction and l the plate length. The natural question which arises is to know whether the rate of the sediment eroded from the plate, Q_e, adjusts itself to the injected sediment rate Q_{in}.

We made a set of calibration experiments to evaluate Q_e as a function of Q_{in}, at a given flow rate of 71 L/min. Q_e is estimated via the height of the bed surface of the sediment supply system. After a short transient, the eroded sediment rate Q_e stabilizes to a stationary value (Fig. 3). We found that the equilibrium value of Q_e adjusts exactly to the imposed sediment rate Q_{in} (Fig. 4). This self-adjustment is possible because the system can adapt the position of the sediment surface in order to increase or decrease

locally the basal shear stress (via a reduction or an augmentation of the flow cross section). In the following, the incoming sediment discharge will be referred to Q_{in}.

Sediment can thus be supplied at a constant and controlled rate at the entrance of the flume. Q_{in} was varied from 0.7 $g.s^{-1}.m^{-1}$ to 14 $g.s^{-1}.m^{-1}$, for a water flow rate of 71 L/mn. As specified earlier, the corresponding shear velocity in the working area is u* = 2.6 cm/s. We can estimate the corresponding satured sediment flow rate using Meyer-Peter and Müller law (Meyer-Peter E. & Müller R. 1948): $Q_{sat} \sim 9\ g.s^{-1}.m^{-1}$. The important point to note is that the range of variation of Q_{in} extends from $0.1 \times Q_{sat.}$ to $2 \times Q_{sat}$.

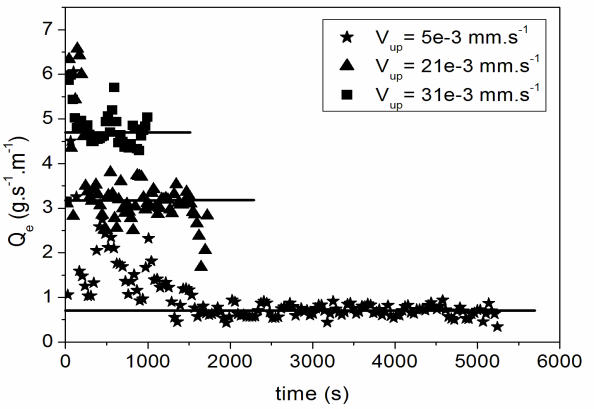

Figure 3. Eroded sediment rate Q_e against time, for different values of the rising velocity V_{up}.

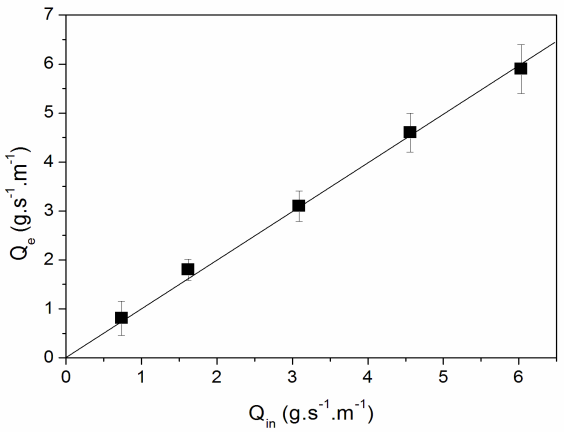

Figure 4. Eroded sediment rate Q_e against injected sediment rate Q_{in}.

3 EXPERIMENTAL RESULTS

We report here two set of experiments made with two different bottom roughnesses: 100 µm and 250 µm. At the beginning of each experiment, the channel substrate is cleaned, and the sediment supply system is filled up with 100 µm grains. A few seconds after the experiment is started (the water flow and the sediment supply system are triggered simultaneously), sediment deposit patterns appear over the rough bottom. The deposits grow and eventually reach an equilibrium (or steady) pattern.

3.1 *Morphological description of the deposits*

Depending on the sediment discharge Q_{in}, two types of morphology appear. For low discharge, deposits are isolated and have a crescentic shape: they look like barchan dunes (Fig. 5a), observed in aeolian case (Bagnold 1941).As Q_{in} increases, deposits are more and more connected and loose their crescentic shape: the crest becomes rectilinear and they look like transverse dunes (Fig. 5b). The transition between barchan dune and transverse dune occurs at $Q_{in} \sim 0.1\ Q_{sat}$. Barchan dunes form therefore within a very narrow range of incoming sediment rate Q_{in}: $0 \leq Q_{in} \leq 0.1\ Q_{sat}$. Additional experiments at different water flow rate are needed to determine whether the critical incoming sediment rate for the morphological transition depends on the flow conditions.

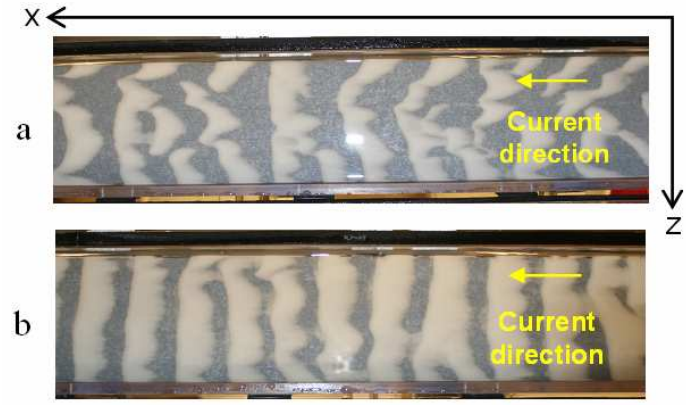

Figure 5. a) At low sediment discharge, barchan dunes form, $Q_{in} \leq 0.1 \times Q_{sat}$. b) At high sediment discharge, transverse dunes develop, $Q_{in} > 0.1 \times Q_{sat}$.

Here, we focus exclusively on the dynamics of the transverse dune patterns which are invariant in the direction perpendicular to the flow. We have measured the surface position, y = h(x,z) of the deposit pattern and its evolution in course of time for different incoming sediment rates.

Figure 6 shows the temporal evolution of the mean height <h> of the deposit. We can observe a transient where the mean height is increasing before it reaches a steady value, denoted $<h>_{eq.}$. It is worth noting that $<h>_{eq}$ is directly proportional to the specific mass (mass per unit surface) of the deposit:

$$M_{dep.} = \rho_{beads} \times \Phi \times < h >_{eq} \qquad (2)$$

where ρ_{beads} is glass beads density and Φ is the solid volume fraction.

The steady (or equilibrium) value $<h>_{eq.}$ is reached faster with increasing sediment rate Q_{in} and

is larger as Q_{in} increases (Fig. 7). We can also note that $<h>_{eq.}$ is independent on the bottom roughness.

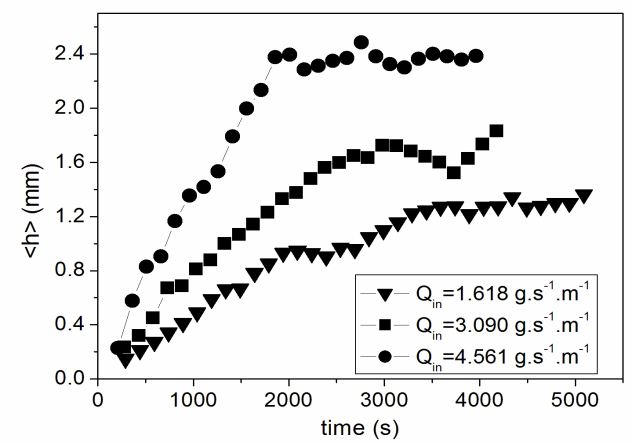

Figure 6. Mean height < h > of the bed forms against time, for three different values of Q_{in}.

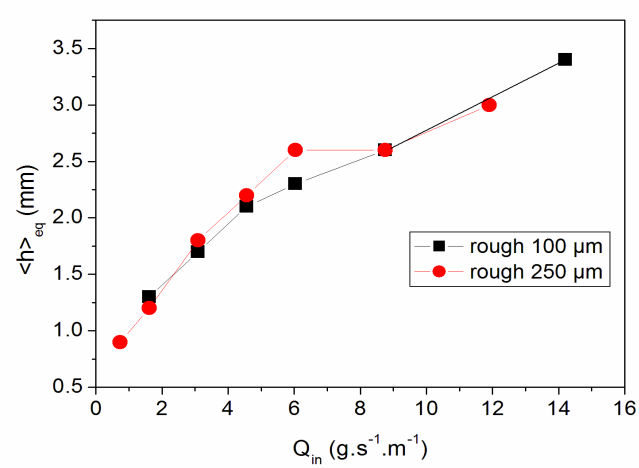

Figure 7. $< h >_{eq}$ against Q_{in} for two bottom roughnesses.

We have also extracted from the surface position, h(x,z), of the deposits several morphological features: the height H of the dunes, their length L, their aspect ratio R = H / L, and the dune spacing λ (Fig. 8).

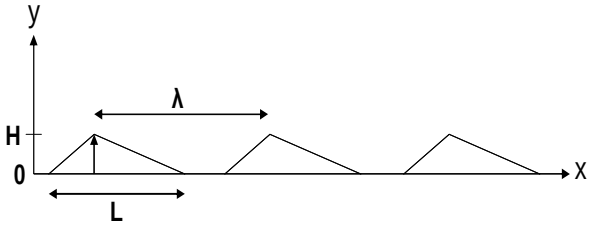

Figure 8. Geometrical parameters characterizing the transverse dunes.

These features are found rather uniform along the downstream direction. Figures 9-11 show the equilibrium value H_{eq}, R_{eq} and λ_{eq} as a function of Q_{in}. H_{eq} (as well as L_{eq} which is not shown here) increases with increasing Q_{in}. However, the aspect ratio R_{eq} decreases with increasing Q_{in}, which indicates that L_{eq} increases at a faster rate than H_{eq}. As a result, the dunes tend to flatten as Q_{in} increases.

Another interesting feature is the coverage rate C of the working area: C = s/S where s is the surface covered by sediments and S the total surface of the working area. C is also related to the interdune spacing reduced by the dune length: C = λ/L. Figure 12 shows the equilibrium value C_{eq} of the coverage rate in the steady regime for different values of Q_{in}. It increases with increasing Q_{in}, but seems to saturate to a value of 80 % when Q_{in} approaches Q_{sat}. If the sediment discharge Q_{in} is increased further, the coverage rate does not increase up to 100 %.

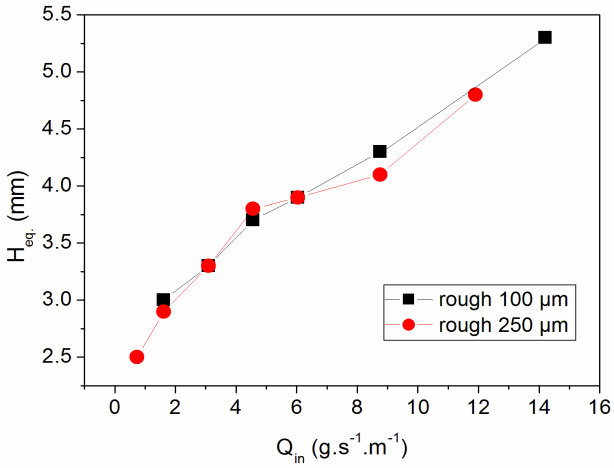

Figure 9. H_{eq} against Q_{in}, for two bottom roughnesses.

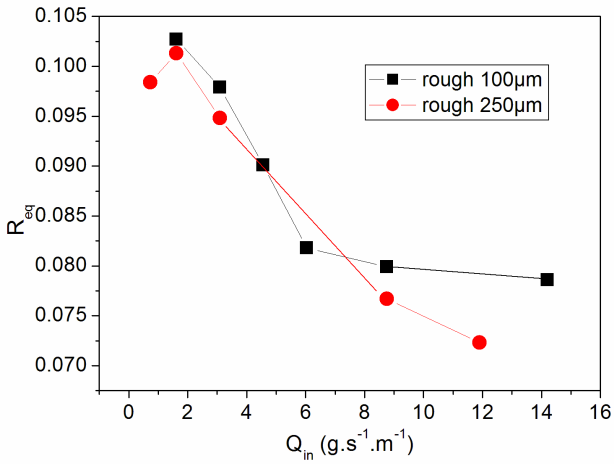

Figure 10. R_{eq} against Q_{in} for two bottom roughnesses.

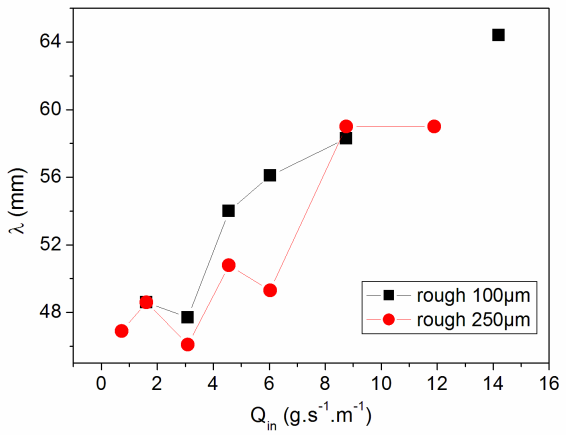

Figure 11. λ_{eq} against Q_{in} for two bottom roughnesses.

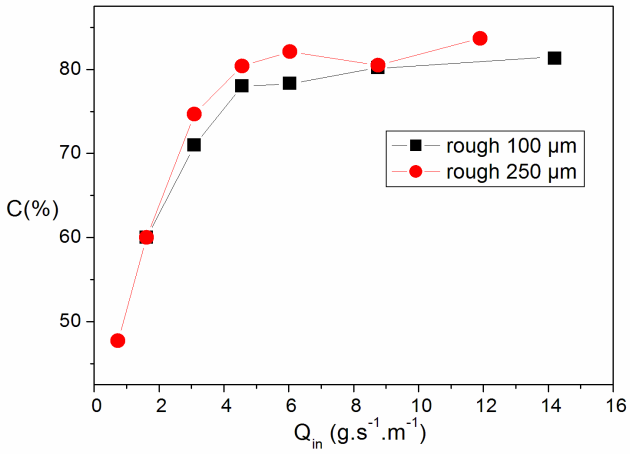

Figure 12. Steady value of the coverage rate C against Q_{in} for two bottom roughnesses.

The last feature analyzed is the migration speed of the deposit pattern. We found a surprising result: the migration speed in the steady regime appears to be independent of Q_{in} (V_{eq} = 0.3 mm.s^{-1}).

3.2 *Evaluation of the different modes of sediment transport*

The total sediment transport rate averaged over the study area can be split in different contributions:

$$< Q_{TOT} > = < Q_D > + < Q_S > + < Q_{BL} > \quad (3)$$

Q_{BL} represents the bedload contribution while Q_S stands for the part of the sediment transported directly by the fluid (suspension). The last contribution Q_D corresponds to the sediment transported by the dunes during their migration. In the steady regime, $<Q_D>$ can be easily estimated from the morphodynamics of the deposits. Indeed, we have:

$$<Q_D> = \rho_{beads} \times \Phi \times V_{eq.} \times < h >_{eq} \quad (4)$$

From the vertical concentration and velocity profiles of the suspended particles, we can calculate the suspended sediment flux Q_S. The bedload contribution to the transport is difficult to evaluate by direct measurements. We estimated indirectly using mass conservation argument. In a steady regime, the total sediment transport rate $< Q_{TOT} >$ averaged over the study area is expected to be equal to the imposed incoming sediment rate Q_{in}: $< Q_{TOT} > = Q_{in}$. Therefore, $<Q_S>$ can calculated as follows:

$$< Q_{BL} > = Q_{in} - < Q_D > - < Q_S > \quad (5)$$

Figure 13 shows the relative contribution of the different modes of sediment transport as a function of the sediment discharge Q_{in}. For low seeded flow, the three different contributions are on the same order of magnitude, while, as Q_{in} increases, the bedload transport prevails over the two other modes.

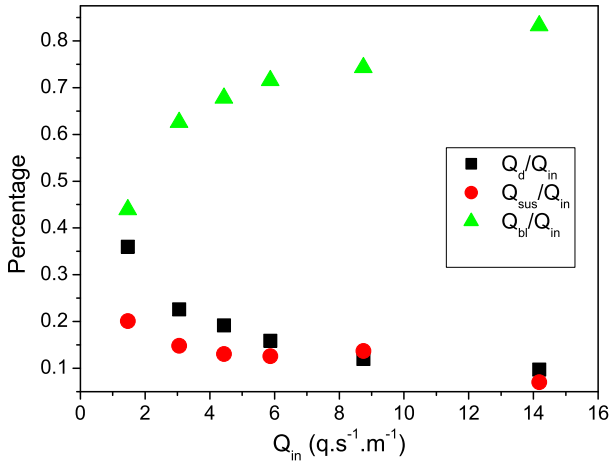

Figure 13. : $< Q_D >$, $< Q_S >$, and $< Q_{BL} >$ (reduced by Q_{in}) against Q_{in}.

4 DISCUSSION AND CONCLUSION

We carried out an experimental study on sediment dynamics in a flume in which the sediment supply rate can be set independently of the water flow rate. We reported measurements both on the bedform dynamics and on the partition between the different modes of transport. We evidenced that the roughness of the bottom has no influence on the bedform dynamics, while the sediment supply rate, in addition to the flow conditions, plays a crucial role in the sediment dynamics.

A surprising observation is the existence of a steady and fully developed state in the whole range of the sediment supply rates investigated so far (from $0.1 \times Q_{sat}$ to $2 \times Q_{sat}$, where Q_{sat} is the saturated sediment rate predicted by the Meyer-Peter and Muller law). It means that the system adapts itself to the imposed sediment supply rate through the variation of

the bedform morphology. Besides, the stationary morphology of the bedforms depends on the sediment supply rate. The height and the spreading of the deposits increase with increasing sediment supply rate.

Another striking result is the observation of a deposition process in conditions where the flow is not saturated in sediments ($Q_{in}<Q_{sat}$). In such conditions, the fluid should be capable of transporting all the sediment supplied and we would have a priori expected an absence of deposits. This is not what it is observed, since at arbitrary small sediment supply rate, deposits always form.

We also showed that the migration speed of the bedforms is independent of the sediment supply rate, although they have various amplitudes. This result contrasts with the case of aeolian bedforms, where the dune migration speed varies as the inverse of the dune height at a given wind shear velocity. Further experiments are needed to determine whether the migration speed of the bedforms depends on the fluid flow rate.

Due to the peculiar setup configuration (absence of free surface), the extrapolation of our results to rivers should be taken with caution. Our results nevertheless suggest that a flow can transport more sediments than what it is predicted by the Meyer-Peter and Muller law. This outcome needs further analysis of the hydraulic conditions in order to understand better the coupling between the flow, the bedform morphology and the sediment transport.

Our future investigations will focus on the modification of the flow conditions due to the presence of the bedforms and on the partition of the different modes of sediment transport according to the fluid flow rate.

5 REFERENCES

Bagnold R. 1941. *The physics of blown sand and desert dunes*. Chapman and Hall, Londres.

Breque C. & Dupre J.-C. & Bremand F. 2004. Calibration of a system of projection Moiré for relief measuring: biomechanical applications. *Optics and Lasers in Engineering* **41**: 241-260.

Charru F. & Mouilleron H. & Eiff O. 2004. Erosion and deposition of particles on a bed sheared by a viscous flow. *J. Fluid Mech.* **519**: 55-80.

Church M. & Hassan MA. & Wolcott J.-F. 1998. Stabilizing self-organized structures in gravel-bed stream channels: field experimental observations. *Water Resour. Res.* **34**: 3169–3179.

Endo N. & Sunamura T. & Takimoto H. 2005. Barchan ripples under unidirectional water flows in the laboratory: formation and planar morphology. *Earth Surf. Process. Landforms.* **30**: 1675-1682.

Langlois V. 2005. Instabilité d'un lit granulaire cisaillé par un écoulement fluide. PhD Thesis.

Meyer-Peter E. & Müller R. 1948. Formula for the bedload transport. *Proceedings of the 3rd Meeting of the International Association of Hydraulic Research*: 39-64.

Ouriemi M. 2007. Erosion, transport et instabilités d'un lit de particules dans un tube. PhD Thesis.

Turowski J. & Lague D. & Hovius N. In press, 2007. The cover effect in bedrock abrasion: a new derivation and its implications for the modeling of bedrock channel morphology. *J. Geophys. Res.- Earth Surface.*